HHS Public Access

Author manuscript

Sci Transl Med. Author manuscript; available in PMC 2024 February 25.

Published in final edited form as:

Sci Transl Med. 2023 August 16; 15(709): eabm5755. doi:10.1126/scitranslmed.abm5755.

Endothelial FoxM1 reactivates aging-impaired endothelial regeneration for vascular repair and resolution of inflammatory lung injury

Xiaojia Huang[1,2,†,‡], **Xianming Zhang**[1,2,†], **Narsa Machireddy**[1,2], **Colin E. Evans**[1,2], **Shawn D. Trewartha**[1,2], **Guochang Hu**[3], **Yun Fang**[4], **Gökhan M. Mutlu**[4], **David Wu**[4,#], **You-Yang Zhao**[1,2,5,6,7,*]

[1]Program for Lung and Vascular Biology and Section for Injury Repair and Regeneration Research, Stanley Manne Children's Research Institute, Ann & Robert H. Lurie Children's Hospital of Chicago, Chicago, IL60611, USA.

[2]Department of Pediatrics, Division of Critical Care, Northwestern University Feinberg School of Medicine. Chicago, IL60611, USA.

[3]Departments of Anesthesiology and Pharmacology, University of Illinois College of Medicine, Chicago, IL60607, USA.

[4]Section of Pulmonary and Critical Care Medicine, Department of Medicine, University of Chicago, Chicago, IL60637, USA.

[5]Department of Pharmacology,

[6]Department of Medicine, Division of Pulmonary and Critical Care Medicine,

[7]Feinberg Cardiovascular and Renal Research Institute, Northwestern University Feinberg School of Medicine. Chicago, IL60611, USA.

Abstract

Aging is a major risk factor of high incidence and increased mortality of acute respiratory distress syndrome (ARDS). Here, we demonstrated that persistent lung injury and high mortality in aged mice after sepsis challenge was attributable to impaired endothelial regeneration and vascular repair. Genetic lineage tracing study showed that endothelial regeneration following sepsis-induced vascular injury was mediated by lung resident endothelial proliferation in young

*Corresponding author. youyang.zhao@northwestern.edu.
†These authors contributed equally.
‡Current address: Institute of Biomedical Engineering and Health Sciences, Changzhou University. Changzhou, Jiangsu, China.
#Current address: Department of Pulmonary/Critical Care, Kaiser Permanente Oakland Medical Center, Oakland, California.

Author Contribution: X.H., X.Z., and Y.Y.Z. conceived the experiments. X.H., X.Z., N.M. C.E.E., S.D.T. designed, carried out experiments, and analyzed the data. X.H., X.Z., Y.Y.Z. analyzed and interpreted the data. G.H. and G.M.M. provided intellectual input. Y.F., and D.W. provided the COVID-19 patient samples and intellectual input. X.H. wrote the manuscript. Y.Y.Z. supervised the project and revised the manuscript and is responsible for the concept.

Competing interests: Y.Y.Z is the founder and chief scientific officer of MountView Therapeutics LLC. This project utilizes technologies subject to the following pending patents PCT/US21/70767 "Methods and compositions for the treatment of COVID-19 and associated respiratory distress and multi-organ failure, sepsis, and acute respiratory distress syndrome, and cardiovascular diseases", and PCT/US2019/055787 "PLGA-PEG nanoparticles and methods of uses" by Zhao, Y.Y. The other authors declare no competing interests.

adult mice whereas this intrinsic regenerative program was impaired in aged mice. Expression of FoxM1, an important mediator of endothelial regeneration in young mice, was not induced in lungs of aged mice. Transgenic *FOXM1* expression or in vivo endothelium-targeted nanoparticle delivery of the *FOXM1* gene driven by an endothelial cell (EC)-specific promoter reactivated endothelial regeneration, normalized vascular repair and resolution of inflammation, and promoted survival in aged mice after sepsis challenge. In addition, treatment with the FDA-approved DNA demethylating agent decitabine was sufficient to reactivate FoxM1-dependent endothelial regeneration in aged mice, reverse aging-impaired resolution of inflammatory injury, and promote survival. Mechanistically, aging-induced *Foxm1* promoter hypermethylation in mice, which could be inhibited by decitabine treatment, inhibited Foxm1 induction after sepsis challenge. In COVID-19 lung autopsy samples, *FOXM1* was not induced in vascular ECs of elderly patients at age of 80s, in contrast to middle aged patients (aged 50–60 years). Thus, reactivation of FoxM1-mediated endothelial regeneration and vascular repair may represent a potential therapy for elderly patients with ARDS.

INTRODUCTION

Acute respiratory distress syndrome (ARDS) is a form of acute-onset hypoxemic respiratory failure with bilateral pulmonary infiltrates that is caused by acute inflammatory edema of the lungs not attributable to left heart failure (1–3). Common causes of ARDS include sepsis, pneumonia, inhalation of harmful substances, burns, major trauma with shock and massive transfusion. Sepsis, with annual U.S. incidence of over 750,000, is the most common cause. Endothelial injury, characterized by persistently increased lung microvascular permeability resulting in protein-rich lung edema, is a hallmark of acute lung injury (ALI) and ARDS (4–7). Despite recent advances in the understanding of the pathogenesis of ARDS, there are currently no effective pharmacological or cell-based treatments of the disease and the mortality remains as high as 40% (1–3). Compared to young adults, the incidence of ARDS resulting from sepsis and pneumonia in the elderly (≥ 65 yr.) is as much as 19-fold greater and mortality is up to 10-fold greater (3, 8–11). However, the underlying causes of the high incidence and mortality of ARDS in the elderly are poorly understood, and little is known about how aging influences mechanisms of endothelial regeneration and resulting restoration of vascular homeostasis.

The forkhead box (Fox) transcriptional factors share homology in the winged helix or forkhead DNA-binding domains (12, 13). Among the Fox family, FoxM1 was the first to be identified as a proliferation-specific transcriptional factor and is expressed during cellular proliferation to control the transcription of many cell cycle genes (14–16). During embryogenesis, FoxM1 is expressed in many types of cells, such as cardiomyocytes, endothelial cells (ECs), hepatocytes, lung epithelium cells, and smooth muscle cells (17–19). In adult mice, FoxM1 expression is restricted to intestinal crypts, thymus and testes (12, 13). Although FoxM1 is silenced in terminally differentiated cells, it can be induced after organ injury: We have previously reported that FoxM1 is induced in lung ECs in the repair phase but not in the injury phase in young adult mice following sepsis challenge (19). In EC-restricted *Foxm1* knockout mice, pulmonary vascular EC proliferation and endothelial barrier recovery are defective following inflammatory injury (19, 20). FoxM1 also promotes

re-annealing of the endothelial adherens junctional complex to restore endothelial barrier function after vascular injury (21). These results demonstrated the importance of FoxM1 in vascular repair. Other studies have also demonstrated important roles for FoxM1 in mediating lung epithelial repair (22) and hepatocyte regeneration (23) in young adult mice. However, it is unknown if FoxM1 can be induced in aged lungs and whether activation of FoxM1 expression alone in pulmonary vascular ECs is sufficient to reactivate endothelial regeneration and vascular repair to resolve inflammatory lung injury in aged mice.

Here we sought to i) define the cells mediating endothelial regeneration in young adult mice, ii) determine how aging affects this process, and iii) delineate the underlying molecular mechanisms. We hypothesized that aging impairs the intrinsic FoxM1-dependent endothelial regeneration and vascular repair program after inflammatory lung injury, and restored expression of FoxM1 alone in lung ECs could reactivate the regenerative program in aged mice. We demonstrated that aging impairs the intrinsic endothelial regeneration program leading to persistent inflammatory lung injury. Restored FoxM1 expression in lung ECs (transgenic or non-viral delivery of plasmid DNA) in aged mice was necessary and sufficient to re-activate lung endothelial regeneration and promote survival after sepsis challenge. Further, the FDA-approved drug decitabine could reactivate FoxM1 expression in aged mice and restore endothelial regeneration and vascular repair and promote survival after endotoxemia or polymicrobial sepsis. Lastly, we demonstrated that aging impaired *Foxm1* expression through methylation of its promoter, which was inhibited by decitabine treatment. Thus, repurposing decitabine to activate FoxM1-dependent endothelial regeneration and vascular repair in aged lungs represents a potential treatment of ARDS in older patients.

RESULTS

Aging impairs intrinsic lung endothelial regeneration after injury induced by polymicrobial sepsis

The major pathogenic feature of ALI and ARDS leading to deterioration of vascular barrier function is the marked loss of ECs (19, 24, 25). To trace the changes of pulmonary ECs after sepsis challenge, we carried out genetic lineage tracing on pulmonary ECs using a tamoxifen-inducible mTmG/*EndoSCL*-Cre^{ERT2} mouse (Fig. 1A).95% of lung ECs ($CD45^{-}CD31^{+}$) were labeled with green fluorescent protein (GFP) whereas < 2.5% of GFP^{+} cells were either $CD45^{+}$ cells (leukocytes) or $CD31^{-}$ cells (non-ECs) (Fig. 1, B and C and fig.S1, A to E). Fluorescence imaging revealed the presence of GFP^{+} ECs in capillaries and along the inner surfaces of blood vessels but not in bronchioles (Fig. 1D). In young adult mice (3–5 mos. old), at 48h after cecal ligation and puncture (CLP), which causes lethal peritonitis and polymicrobial sepsis, a clinically relevant murine model of sepsis (26, 27), the presence of GFP^{+} ECs was disrupted along the blood vessel inner surfaces and also the alveoli, consistent with loss of ECs seen in patients and animal models (fig. S2); TUNEL staining further confirmed loss of ECs of both large and medium-sized vessels and small vessels/capillaries (fig. S3, A and B), H & E staining showed disrupted alveolar structure and cell infiltrates (fig.S5, A to C). By 144h after CLP, the blood vessel inner wall was lined with GFP^{+} ECs again (fig. S2A).

To quantify the changes of pulmonary EC numbers over the course of sepsis-induced injury and recovery, we measured the percentage of $CD45^{-}GFP^{+}$ cells in the whole lung by fluorescence-activated cell sorting (FACS) in young adult mice. In sham animals, about 40% of pulmonary $CD45^{-}$ cells were GFP^{+}. At 48h after CLP, this number had dropped to 25%, but was followed by a steady return to baseline percentages by 144h (Fig. 1, E and F). However, the $CD45^{+}GFP^{+}$ cell population remained at minimal percentages at various times (fig. S5), indicating that $CD45^{+}GFP^{+}$ cells were not directly contributing to endothelial regeneration.

To further determine whether bone marrow-derived cells contributed to endothelial regeneration after sepsis, we transplanted bone marrow cells from mTmG/*EndoSCL*-Cre^{ERT2} mice into lethally irradiated WT mice (8 weeks old) to generate chimeric mice. We observed a small population (<0.1%) of $CD45^{-}GFP^{+}$ cells in the chimeric mouse lungs (Sham group, 14 weeks old). At 144h after CLP, the percentage of this cell population was unaltered (fig. S6A). The $CD45^{+}GFP^{+}$ population also remained steady (fig. S6B). Thus, bone marrow-derived cells were not directly responsible for lung endothelial regeneration. Together the data of Fig. 1, E and F and fig. S6, A and B demonstrated that lung resident ECs are the major cell source for endothelial regeneration in adult mice following inflammatory vascular injury.

FACS analysis revealed that the lung GFP^{+} EC population was markedly decreased at 48h post-CLP in aged (19–21 mos.) mice as observed in young adult mice. However, in contrast to young adult mice (Fig. 1F), the GFP^{+} EC population in aged mice failed to recover and remained low at 144h after CLP (Fig. 1G and fig. S2B). Thus, aging was associated with an impaired intrinsic endothelial regeneration program after sepsis-induced injury.

Impaired endothelial regeneration leads to persistent inflammatory lung injury in aged mice after polymicrobial sepsis

Anti-BrdU immunostaining, indicative of cell proliferation, revealed defective lung endothelial proliferation in aged mice in contrast to young adult mice during the recovery phase (at 72 and 96h after CLP) (Fig. 2, A and B). Accordingly, an Evans blue-conjugated albumin (EBA) assay, a measurement of vascular permeability to protein, showed persistent vascular leak indicating impaired vascular repair in the lungs of aged mice whereas vascular permeability was returned to basal amounts at 96h after CLP in young adult mice (Fig. 2C). The aged lungs also exhibited marked edema measured by greater lung wet-to-dry weight ratios at 72h after CLP (Fig. 2D) and impaired resolution of inflammation during the recovery phase, evident by persistently elevated lung myeloperoxidase (MPO) activity (Fig. 2E), indicative of neutrophil sequestration, and increased expression of proinflammatory cytokines in lung tissue (Fig. 2F). Consistently, all aged mice died within 100h of severe CLP challenge whereas all young adult mice survived during this time (Fig. 2G).

Aging impairs lung vascular repair and resolution of inflammation in mice after endotoxemia

To determine if aged mice also exhibit impaired vascular repair following endotoxemia, aged (19–21 mos.) and young (3–5 mos.) mice were challenged with lipopolysaccharide (LPS).

Because aged mice exhibited greater lung injury as indicated by greater EBA flux and MPO activity at 24h after LPS compared to young adult mice in response to the same dose of LPS, we challenged aged mice with a lower dose of LPS (1.0 mg/kg) to induce a similar degree of vascular injury during the injury phase (at 24h after exposure) as seen in young adult mice with 2.5 mg/kg of LPS (Fig. 3A). EBA flux in young adult mice was reduced at 48h and returned to baseline amounts at 72h after LPS, whereas it remained elevated at these times in aged lungs, consistent with defective vascular repair (Fig. 3A). Aged lungs exhibited edema at 72h after LPS, which was not observed in young adult mice (Fig. 3B). We also collected bronchoalveolar lavage fluid (BALF) to assess protein permeability and cell infiltration including macrophages (fig. S7, A to C). Although similar protein leakage and cell infiltration were observed at 24h after LPS in young and aged mice, BALF protein concentrations and cell counts returned to baseline in young adult mice at 96h after LPS, but not in aged mice. Together, these data support the notion of defective vascular repair in aged lungs.

MPO activity was similarly increased versus basal controls at 24h after LPS in young adult and aged mice (Fig. 3C). Although MPO activity returned to baseline in lungs of young adult mice at 72h after LPS, it remained elevated in aged lungs (Fig. 3C). H & E staining showed similar degrees of injury at 24h after LPS in young and aged mouse lungs (Fig. 3D). However, at 96h, lung structure and cellular infiltrates were largely normalized in young mice whereas they remained abnormal in aged mice (Fig. 3D). Together, these data demonstrated impaired resolution of inflammation in aged lungs after LPS challenge.

To further determine how aging affected vascular repair and inflammation resolution, we challenged the mice at various ages (from 3 to 21 mos. old) with LPS and assessed EBA flux and MPO activity at 72h after LPS. EBA flux in mice at age of 9 mos. or younger returned to baseline but not in 12 mos. old mice which maintained EBA flux at a marginally increased amount. EBA flux was elevated in 15 mos. old mice and markedly elevated in aged mice (18 and 21 mos. old) (Fig. 3E). We also observed similar changes in MPO activity. Lung MPO activity did not return to baseline at 72h after LPS in mice at age 12 mos. or younger and remained markedly increased in lungs of mice at age 15 mos. or older, indicating impaired resolution of inflammation (Fig. 3F). Thus, mice at age 18 mos. or older exhibited markedly impaired vascular repair and diminished resolution of inflammatory lung injury.

Defective endothelial proliferation and inhibited FoxM1 induction in aged lungs following LPS challenge

To gain insights into the molecular and cellular mechanisms of impaired vascular repair and inflammation resolution in aged lungs, we first determined lung endothelial proliferation by in vivo BrdU labeling. There was a marked increase of endothelial proliferation in the lungs of young adult mice at 72h after LPS whereas endothelial proliferation in lungs of aged mice was largely inhibited (Fig. 4, A and B), indicating impaired endothelial regeneration in aged lungs. Because FoxM1 is a critical reparative transcriptional factor (19, 22, 23), we assessed *Foxm1* expression in mouse lungs. *Foxm1* mRNA was markedly induced in the lungs of young adult mice during the recovery phase (at 48 and 72h) but not in the injury phase, (24h

after LPS). However, *Foxm1* was not induced in aged lungs after LPS challenge (Fig. 4C). Accordingly, FoxM1 target genes essential for cell cycle progression such as *Cell division cycle 25C* (*Cdc25c*), and *Cyclin A2* (*Ccna2*) were not induced in aged lungs (Fig. 4D). In young adult mice, *Foxm1* expression and its transcriptional target genes peaked at 3–4 days after LPS challenge and then gradually decreased near baseline at 8 days post-LPS (Fig. 4, C and D, and fig. S8, A and B).

Normalized vascular repair and inflammation resolution in aged *Foxm1^{Tg}* mice.

To determine if failure of FoxM1 induction is responsible for the impaired vascular repair and inflammation resolution seen in aged mice, we employed *FOXM1^{Tg}* mice expressing human *FOXM1* under the control of the 800-base pair *Rosa26* promoter (28). EBA flux was similar under basal conditions and increased similarly at 24h after LPS in aged *FOXM1^{Tg}* mice compared to aged WT mice, demonstrating similar degrees of lung vascular injury (Fig. 5A). EBA flux was then reduced at 48h and returned to an amount close to baseline at 72h after LPS in aged *FOXM1^{Tg}* mice whereas it was persistently elevated in aged WT mice (Fig. 5A). MPO activity was similarly increased during the injury phase in aged WT and *FOXM1^{Tg}* mice. MPO activity was reduced during the recovery phase and returned to baseline at 72h after LPS in aged *FOXM1^{Tg}* mice but not in aged WT mice (Fig. 5B). Expression of proinflammatory genes *Tnf* and *Il6* was markedly elevated in aged WT mice but not in aged *FOXM1^{Tg}* mice (fig. S9, A and B). These data demonstrate resolution of inflammation in aged *FOXM1^{Tg}* mice in contrast to aged WT mice after LPS challenge. Accordingly, lung endothelial proliferation in aged *FOXM1^{Tg}* mice was activated at 72h after LPS, in contrast to aged WT mice (fig. S10, A and B).

To determine effects on survival, aged mice were challenged with a higher dose of LPS (1.5 mg/kg). Although 100% of young WT mice survived, aged WT mice exhibited 100% mortality within 3 days (Fig. 5C). We also observed a 50% mortality with 1 mg/kg of LPS at 96h after LPS challenge (fig. S11). However, 70% of aged *FOXM1^{Tg}* mice survived to 7 days after LPS challenge (1.5 mg/kg) (Fig. 5C).

Nanoparticle-directed FoxM1 expression in the endothelium of the lung normalizes endothelial regeneration and resolution of inflammatory lung injury in aged WT mice

Next, we employed an endothelium-targeted nanoparticle gene delivery approach (29) to determine if forced FoxM1 expression in lung vascular ECs of aged WT mice could reactivate endothelial proliferation and thus reverse the defective resolution of inflammatory lung injury. A mixture of nanoparticles:plasmid DNA expressing human *FOXM1* under the control of human *CDH5* promoter (EC-specific) was administered retro-orbitally to 19–20 mos. old WT mice at 24h after LPS challenge (established lung injury). Empty vector DNA was administered to a separate cohort of aged and gender-matched WT mice. As shown in Fig. 5D and fig. S12, nanoparticle delivery of *FOXM1* plasmid DNA resulted in a marked increase of Foxm1 mRNA and FoxM1 protein expression in aged WT mice at 72h after LPS compared to mice receiving empty vector DNA. This increase was comparable to FoxM1 expression in young adult mice (Fig. 5D). EBA flux was decreased in *FOXM1* plasmid DNA-administered mice compared to vector DNA-administered mice (Fig. 5E). Lung MPO activity returned to baseline in *FOXM1* plasmid DNA-administered mice (Fig. 5F).

We also assessed whether the restored vascular repair and resolution of inflammation was attributable to reactivated endothelial regeneration in aged lungs. BrdU labeling studies revealed an increase of EC proliferation in lungs of *FOXM1* plasmid DNA-administered mice in contrast to vector DNA-administered mice (Fig. 5, G and H). Expression of FoxM1 target genes including *Cdc25c*, *Cyclin D2* (*Ccnd2*), and *Cyclin F* (*Ccnf*) (15) was also markedly induced in the lungs of *FOXM1* plasmid DNA-administered aged mice (Fig. 5I). Expression of angiogenic factor *Fgf1* and of endothelial adherens junction proteins VE-Cadheren (*Cdh5*) and β-catenin (*Ctnnb1*) was markedly increased in lungs of young adult mice but not in aged mice at 72h post-LPS (fig. S13, A to F). However, restored FoxM1 expression in aged lungs led to increased expression of these genes (fig. S13).

To further determine if restoration of FoxM1 expression selectively in pulmonary vascular ECs was sufficient to reactivate lung endothelial regeneration and vascular repair in aged mice, plasmid DNA expressing *FOXM1* under the control of a lung EC-specific promoter system comprised of the dual *Cdh5*/*Tmem100* promoters (fig. S14A) was delivered to aged mice 24h after LPS. Quantitative RT-PCR analysis demonstrated marked increases of *FOXM1* expression and its transcriptional target genes *Cdc25c* and *Ccna2* in lungs of *FOXM1* plasmid DNA-administered aged mice compared to vector DNA-administered mice at 72h post-LPS (fig. S14, B to D). EBA flux and MPO activity as well as expression of the proinflammatory genes *Il6* and *Tnf* in lungs of *FOXM1* plasmid DNA-administered aged mice at 72h after LPS were markedly reduced (fig. S14, E to H).

Decitabine reactivates FoxM1-dependent endothelial regeneration and vascular repair in the lungs following endotoxemia in aged mice

We next explored the possibility of pharmacological activation of FoxM1-dependent endothelial regeneration in aged murine lungs. Given the important role of epigenetics in aging, we focused on the DNA methyl transferase inhibitor decitabine and histone deacetylase inhibitor (trichostatin A). In a preliminary study, we observed that 5-Aza 2'-deoxycytidine and trichostatin A treatment but not trichostatin A alone could normalize EBA flux and MPO activity in aged mice after LPS challenge (fig. S15, A and B). Thus, we used decitabine in the following experiments. At 24h and 48h after LPS challenge, aged (21–22 mos. old) mice were treated with decitabine (0.2 mg/kg, i.p.) or vehicle (PBS) and lung tissues were collected at 96h after LPS for analyses. As shown in Fig. 6A, *Foxm1* expression was markedly induced in the lungs of decitabine-treated mice compared to vehicle-treated mice. EBA flux normalized in decitabine-treated mice (Fig. 6B). Lung MPO activity of decitabine-treated mice also returned to baseline whereas vehicle-treated mice exhibited elevated MPO activity (Fig. 6C). However, decitabine treatment did not promote vascular repair in young adult mice at either 52h or 72h after LPS (fig. S16, A and B). ELISA revealed reductions of TNF-α and IL6 protein concentrations in the lungs of decitabine-treated aged mice at 96h after LPS compared to vehicle-treated mice (fig. S17, A and B).

BrdU immunostaining revealed that pulmonary vascular EC proliferation was markedly increased in decitabine-treated aged mice, suggesting reactivation of endothelial regeneration (Fig. 6, D and E). Accordingly, expression of FoxM1 target genes (*Ccna2*,

Ccnf, and *Cdc25c*) essential for cell cycle progression was also induced in the lungs of decitabine-treated aged mice (Fig. 6F). Decitabine treatment also markedly improved survival of aged WT mice. 80% of decitabine-treated mice survived to 96 hours whereas only 20% of vehicle-treated WT mice survived at the same period (Fig. 6G).

To determine if the regenerative and reparative effects of decitabine were mediated by endothelial expression of FoxM1, we employed mice with EC-specific knockout of *Foxm1* (*Foxm1* CKO) (19, 21). As shown in fig. S18A, *Foxm1* expression was induced in the lungs of decitabine-treated aged WT mice at 96h after LPS but not in decitabine-treated *Foxm1 CKO* mic. Expression of the FoxM1target genes (*Ccna2, Ccnf,* and *Cdc25c*) was not induced in decitabine-treated *Foxm1 CKO* lungs (fig. S18, B to D). Lung EBA flux was markedly elevated at 96h after LPS in decitabine-treated aged *Foxm1 CKO* mice whereas it returned to almost baseline in decitabine-treated aged WT mice (24 mos. old) (Fig. 6H). Decitabine-induced resolution of inflammation in aged WT mice was also impaired in aged *Foxm1* CKO mice, as indicated by elevation of lung MPO activity (Fig. 6I) and expression of the proinflammatory cytokine genes *Il6* and *Tnf* (fig. S19). Decitabine treatment did not promote survival of aged *Foxm1* CKO mice following LPS challenge in contrast to aged WT mice (Fig. 6J).

Decitabine reactivates FoxM1-dependent endothelial regeneration and vascular repair in the lungs following polymicrobial sepsis in aged mice

We next determined the effects of decitabine treatment on reactivating endothelial regeneration and vascular repair in aged lungs following polymicrobial sepsis induced by CLP. At 96h after CLP, lung EBA flux was elevated in PBS-treated aged WT mice compared to sham mice whereas decitabine treatment reduced EBA flux (Fig. 7A). Decitabine treatment also improved resolution of inflammation in aged WT mice by reducing MPO activity and mRNA expression of *Tnf* and *Il6* (Fig. 7, B and C). BrdU labeling studies also revealed induction of endothelial proliferation in decitabine-treated aged WT mice at 96h after CLP (Fig. 7, D and E). *Foxm1* mRNA and FoxM1 protein, as well as the mRNA and protein expression of its target Cdc25C and mRNA expression of *Ccna2* were also upregulated in the lungs of decitabine-treated aged WT mice (Fig. 7F, and fig. S20). Decitabine treatment also had marked survival effect on aged WT mice following CLP challenge. Seventy percent of decitabine-treated mice survived at 7 days after CLP compared to only 10% of vehicle-treated mice (Fig. 7G).

We next determined whether decitabine-activated endothelial regeneration and vascular repair in aged WT mice after polymicrobial sepsis was also mediated by reactivation of endothelial FoxM1 expression. Due to the limited availability of *Foxm1 CKO* mice, we employed endothelium-targeted nanoparticles (29) to deliver the CRISPR/Cas9 system to aged WT mice to knockout *Foxm1* in ECs. A mixture of nanoparticles:plasmid DNA expressing Cas9 under the control of *CDH5* promoter and *Foxm1*-specific guide RNA (gRNA) (or control scrambled RNA) was administered to 20–21 mos. old WT mice. 7 days later, lung tissues were collected for cell isolation. Western blotting demonstrated a decrease of FoxM1 protein in lung ECs isolated from gRNA plasmid-administered mice compared to scrambled RNA plasmid mice (fig. S21A). 7 days after nanoparticles:plasmid

administration, the mice were subjected to CLP or sham surgery and then treated with either decitabine or PBS at 24 and 48h after CLP. At 96h after CLP, lung tissues were collected for analyses. Expression of FoxM1 target genes such as *Ccna2* and *Cdc25c* was markedly induced in the lungs of decitabine-treated scrambled RNA plasmid-administered WT mice, but was inhibited in *Foxm1* gRNA plasmid-administered mice (fig. S21, B and C). EBA flux was markedly increased in *Foxm1* gRNA plasmid-administered mice compared to scrambled RNA plasmid mice (Fig. 7H). Decitabine-activated resolution of lung inflammation seen in aged WT mice with scrambled RNA plasmid was impaired in *Foxm1* gRNA plasmid mice (Fig. 7, I to K). Together, these data demonstrate that decitabine-activated vascular repair and resolution of inflammation in aged WT mice following polymicrobial sepsis is also mediated by induced endothelial FoxM1 expression.

Aging impairs FoxM1 expression via hypermethylation of the *Foxm1* promoter in mice and humans.

To gain insights into the molecular mechanism of decitabine reactivation of FoxM1 expression in aged lungs, we addressed the hypothesis that aging impairs FoxM1 expression through hypermethylation of *Foxm1* promoter and decitabine treatment normalizes *Foxm1* promoter methylation. MethPrimer analysis predicted a major CpG island near the transcription start site (Fig. 8A). The CpG island is highly conserved between mouse and human promoters (Fig. 8A). Employing methylation-specific high-resolution DNA melting assay, we observed hypermethylation of the CpG island in lungs of aged mice compared to young adult mice at basal (Fig. 8B).

The CpG island methylation was further increased in LPS-challenged aged mice (Fig. 8C). However, decitabine treatment abrogated hypermethylation of the CpG island in LPS-challenged aged mice (Fig. 8C).

We also collected lung autopsy samples from patients with COVID-19 (Table S1) and carried out RNAscope in situ hybridization assay to determine *FOXM1* expression. *FOXM1* expression in pulmonary vascular ECs was induced in 50–60 years old patients with COVID-19 but not in those over 8 years old (Fig. 8, D and E).

DISCUSSION

Here we demonstrated that in young adult mice, lung resident ECs mediate endothelial regeneration responsible for vascular repair and inflammation resolution after inflammatory injury induced by polymicrobial sepsis. However, aging impairs these processes leading to persistent inflammatory lung injury and high mortality in aged mice with sepsis induced by either LPS or CLP. Mechanistically, aging caused *Foxm1* promoter hypermethylation, inhibiting FoxM1-dependent endothelial regeneration. Forced expression of FoxM1 by transgene or plasmid DNA transiently delivered by endothelium-targeted nanoparticles normalized vascular repair and resolution of inflammation and promoted survival in aged mice. Decitabine treatment reactivated FoxM1-dependent endothelial regeneration leading to improved vascular repair and inflammation resolution and survival in aged mice with sepsis. In patients with COVID-19 who were over the age of 80 years, *FOXM1* expression was not induced in pulmonary vascular ECs, in contrast to those aged 50–60 years. Thus, activation

of FoxM1 expression by repurposing decitabine or endothelium-targeted gene delivery, may represent a potential approach for the treatment of ARDS in elderly patients.

Studies have demonstrated that endothelial barrier dysfunction is a major contributor to lung injury and poor prognostic outcomes of sepsis and ARDS (4, 5, 30–33). Employing genetic lineage tracing and FACS analysis, we showed that the total number of lung ECs decreased from 40% to 25% (a 40% reduction) at 48h after CLP (peak of injury), and returned to baseline at 144h after CLP in young adult mice. A bone marrow transplantation study excluded the potential contribution of engraftment of bone marrow-derived cells to the lung vasculature in this regenerative process. Consistent with our observations, several studies have shown that total number of pulmonary vascular ECs transiently decreased in mice after sepsis challenge (24, 25, 27, 34, 35) and that resident ECs are the major contributor to repair while bone marrow-derived endothelial precursor cells are minor complementary sources of new ECs in endothelial barrier restoration after LPS challenge (36). The caveat of this study is that ECs were labeled with GFP controlled by the constitutively active *Tie2* promoter which is also expressed in hematopoietic cells (37). A recent study employing inducible EC-specific labelling similar to our approach (but without the complementary bone marrow transplantation study) has shown evidence of lung resident EC as the cell source of endothelial regeneration following LPS challenge (38).

An important finding of our study was the identification of the cellular mechanism of aging as a major risk factor of ARDS development and high mortality. Our genetic lineage tracing study demonstrated impaired endothelial regeneration in aged lungs in contrast to young adult mice. We found that mice starting at age of 12 months old exhibited defective vascular repair and inflammation resolution which became more severe with aging. These data could help explain the clinical observations that the incidence and mortality of ARDS resulting from sepsis, pneumonia, and COVID-19 in elderly patients was much greater than young adult patients (8–11, 39, 40). Our data demonstrated failed induction of *FOXM1* expression in patients with COVID-19 who were over 80 years old compared to those aged 50–60 years. Mechanistically, we showed that aging induces hypermethylation of *Foxm1* promoter in a CpG island near the transcriptional start site, which is conserved between mouse and human.

We have shown previously that FoxM1 is markedly induced in ECs in the recovery phase but not in the injury phase in young adult mice after LPS challenge (19). Genetic deletion of *Foxm1* in ECs impaired endothelial proliferation and vascular repair (19). Here we showed that FoxM1 was not induced in aged lungs after sepsis challenge. The failure of FoxM1 induction likely plays a causal role in aging-impaired endothelial regeneration and resolution of inflammatory injury because transgenic expression of FoxM1 prevented the defective phenotype in aged $FOXM1^{Tg}$ mice and promoted survival following LPS challenge. Because FoxM1 was expressed ubiquitously in all cells in the $FOXM1^{Tg}$ mice by the *Rosa26* promoter, it is unknown if the beneficial effects were mediated by FoxM1-dependent endothelial regeneration in aged lungs. Genetic compensation of *FOXM1* overexpression in $FOXM1^{Tg}$ mice may also contribute to the normalized vascular repair in aged mice. Thus, we designed a gene therapy-like approach to determine if transient expression of *FOXM1* in ECs delivered after vascular injury could reactivate the intrinsic

endothelial regeneration program in aged mice. Transient expression of endothelial *FOXM1* in aged lungs did reactivate the intrinsic endothelial regeneration program and normalize the resolution of inflammatory lung injury in aged mice.

Based on our findings in aged mice, we suggest that the FDA-approved drug decitabine may have a role in the treatment of ARDS in older patients. Our data has further demonstrated that the regenerative and reparative effects of decitabine in aged mouse lungs were mediated by induction of endothelial *Foxm1* expression because decitabine failed to reactivate endothelial regeneration or resolve inflammation in aged *Foxm1 CKO* mice following LPS challenge and in aged WT mice with EC-specific disruption of *Foxm1* following CLP challenge. However, decitabine treatment had no effects on vascular repair in young adult mice. A published study has also shown that 5'-Aza 2'-deoxycytidine alone has no protective effects on LPS-induced lung injury in young adult mice (41). Our data support the role of low-dose decitabine in reactivating the aging-impaired FoxM1-dependent endothelial regeneration program for vascular repair and inflammation resolution in aged mice. Decitabine is under a clinical trial to test its safety and efficacy in treating patients with severe COVID-19 (NCT04482621). Our studies suggest that the decitabine dose could be further lowered to possibly improve the safety profile, and the patient population should be focused on elderly patients because decitabine has limited protective role in young adult mice. Because *FoxM1* is also an oncogene, unwanted induction of FoxM1 in other cell types by decitabine treatment may be a cause for concern which will require further study. Thus, endothelium-targeted nanoparticle delivery of the *FOXM1* gene selectively to ECs may be safer.

The study here employed two sepsis models causing indirect lung injury. It is unknown if restored expression of endothelial FoxM1 will activate endothelial regeneration and vascular repair in aged mice following direct lung injury induced by either intratracheal LPS instillation, pneumonia, or COVID-19. Our study focused on endothelial cells, and the role of decitabine treatment in reactivating FoxM1 expression in alveolar epithelial cells, especially type II epithelial cells (42), for epithelial repair in aged lungs requires further study. Another limitation of the study is the lack of large animal models, which may limit the extrapolation of our findings to humans. Although the clinical relevance of our findings is supported by data from lung autopsy samples of COVID-19 patients, interpretation of the results is limited by small sample size.

In summary, we have shown that aging impairs the resolution of inflammatory lung injury following sepsis challenge through induction of *Foxm1* promoter hypermethylation and inhibition of FoxM1-dependent endothelial regeneration and vascular repair. Activation of FoxM1 in lung vascular ECs, through administration of either decitabine or EC-targeted nanoparticles carry FOXM1, could reactivate the intrinsic endothelial regeneration program to improve resolution of inflammatory injury in aged lungs.

MATERIALS AND METHODS

Study design:

This study was designed to delineate the molecular and cellular mechanisms of persistent inflammatory lung injury and higher mortality in aged mice following sepsis challenge and identify effective drug(s) targeting the underlying mechanisms for treatment of ARDS. To accomplish this, we employed a genetic lineage tracing approach coupled with FACS analysis to define the cell source of origin responsible for endothelial regeneration following polymicrobial sepsis in mice. A time course of the changes of genetically labeled lung ECs in young adult (3–5 mos.) and aged (19–21 mos.) mice were studied. For all experiments, male and female mice were studied. Anti-BrdU and anti-CD31 immunostaining were employed to quantify EC proliferation in mouse lungs, indicative of endothelial regeneration. Lung vascular permeability was determined by EBA assay whereas lung edema was assessed by lung wet/dry weight ratio. Lung inflammation was determined by MPO activity and expression of proinflammatory genes. Lung injury was also assessed by H & E staining and BALF protein and cells. Two complementary mouse sepsis models (intraperitoneal LPS and CLP) were used. Both age groups and genders were studied (n=4–5 each group each time point). To delineate the molecular mechanism responsible for the impaired endothelial regeneration and vascular repair of aged lungs, we employed both *FOXM1* transgenic mice and endothelium-targeted nanoparticle delivery of plasmid DNA to induce FoxM1 expression in lung ECs of aged mice after sepsis-induced injury. To address the possibility of activation of endothelial regeneration and vascular repair in aged lungs by epigenetic modifiers, we carried out a pilot study with a DNA methyltransferase inhibitor (5-Aza 2'-deoxycytidine), and a histone deacetylase inhibitor (trichostatin A) which led us to focus on decitabine. We selected a lower and potentially safer dose (.2 mg/kg) than used clinically and administered intraperitoneally the drug to aged mice (20–24 months.) after established injury to reverse injury and thus promote recovery. Aged *Foxm1* EC-specific knockout mice or nanoparticle-targeted CRISPR knockdown of endothelial *Foxm1* in aged mice were employed to define the molecular basis of Decitabine-mediated regenerative and reparative effects. *Foxm1* EC-specific knockout mice and aged WT mice were C57BL/6 background although some of them were not littermates. MethPrimer analysis was employed to identify CpG islands for potential methylation followed by methylation-specific high-resolution DNA melting assay. To address human relevance, we analyzed *FOXM1* expression by RNAscope in situ hybridization in lung autopsy samples from non-surviving patients with COVID-19. Based on the availability of human samples, we examined lungs of 3 male and female middle-aged patients (50–60 years old) and 3 elderly patients (over 80 years old). Fifteen 63× fields each section were randomly selected and quantification was blinded. Sample sizes for the preclinical studies were adequately powered to observe the effects on the basis of past experience (19–21, 30) and preliminary studies. Immunostaining, digital microscopy and imaging were performed blinded to genotype and age. All the data collection and the quantification were performed by investigators unaware of sample identities until unblinding for final interpretation of statistical results. A minimum of n=3 biological replicates were conducted for each experiment.

Mice.

EndoSCL-Cre^{ERT2}/mTmG lineage tracing mice were generated by breeding mice carrying a double-fluorescent reporter expressing membrane-targeted tandem dimer Tomato (mT) prior to Cre-mediated excision and membrane-targeted green fluorescent protein (mG) after excision (mTmG mice, #007676, the Jackson Laboratory) with *EndoSCL*-Cre^{ERT2} transgenic mice (C57BL/6 background) containing tamoxifen-inducible Cre-ERT2 driven by the 5' endothelial enhancer of the stem cell leukemia locus (43, 44). *FOXM1* transgenic (*FOXM1*^{Tg}) mice expressing human *FOXM1* under the control of the *Rosa26* promoter were described previously (28). *Foxm1 CKO* mice with *Tie2*Cre-mediated disruption of *Foxm1* was described previously (19). Both male and female mice were used in the experiments. Mice at various ages (3–5 month-old mice are referred as young adult; 19–24 month-old mice are referred as aged) were used. The experiments were conducted according to NIH guidelines and ARRIVE guidelines on the use of laboratory animals. The animal care and study protocols (IS00006964, IS00020196, A14–168) were approved by the Institutional Animal Care and Use Committees of Northwestern University and The University of Illinois at Chicago.

Human specimens.

All experiments with human tissue samples were performed under protocols approved by the Institutional Review Boards at the University of Chicago and Ann & Robert H. Lurie Children's Hospital of Chicago. Postmortem lung samples were collected from deceased patients with COVID19. Control lung tissues from unused healthy donors were provided by Pulmonary Hypertension Breakthrough Initiative (PHBI).

Statistical analysis.

Statistical significance was determined by one-way analysis of variance (ANOVA) with a Tukey's or Dunette's post hoc analysis for equal variance or Kruskal-Wallis test for unequal variance using Prism 8 (Graphpad Software, Inc. P values were corrected for multiple comparisons. Two-group comparisons were analyzed by the unpaired 2-tailed *t* test for equal variance or by Mann Whitney test for unequal variance. Exclusion criteria that the difference from the mean is >2 stdev was preestablished. No data was excluded in this study. Statistical analysis of the survival study was performed with the log-rank (Mantel-Cox) test. $P < 0.05$ denoted the presence of a statistically significant difference. All bars in dot plot figures represent means.

Supplementary Material

Refer to Web version on PubMed Central for supplementary material.

Funding:

This work was supported in part by NIH grants R01HL123957 to YYZ, R01HL125350 to YYZ, R01HL133951 to YYZ, R01HL140409 to YYZ, R01HL148810 to YYZ, R01HL162299 to YYZ, and R01HL164014 to YYZ; R00HL145113 to DW.

Data and Materials Availability:

All the data used for this study are present in the paper or the Supplementary Materials. The mouse models are available by contacting YYZ with signed Material Transfer Agreement (MTA).

REFERENCES AND NOTES

1. Matthay MA, Ware LB, and Zimmerman GA, The acute respiratory distress syndrome. J Clin Invest. 122, 2731–2740 (2012). [PubMed: 22850883]
2. Matthay MA, Zemans RL, Zimmerman GA, Arabi YM, Beitler JR, Mercat A, Herridge M, Randolph AG, and Calfee CS, Acute respiratory distress syndrome. Nat Rev Dis Primers. 5, 18 (2019). [PubMed: 30872586]
3. Rubenfeld GD, Caldwell E, Peabody E, Weaver J, Martin DP, Neff M, Stern EJ, and Hudson LD, Incidence and outcomes of acute lung injury. N Engl J Med. 353, 1685–93 (2005). [PubMed: 16236739]
4. Aird WC, The role of the endothelium in severe sepsis and multiple organ dysfunction syndrome. Blood. 101, 3765–77 (2003). [PubMed: 12543869]
5. Goldenberg NM, Steinberg BE, Slutsky AS, and Lee WL, Broken barriers: a new take on sepsis pathogenesis. Sci Transl Med. 3, 88ps25 (2011).
6. Lee WL and Slutsky AS, Sepsis and endothelial permeability. N Engl J Med. 363, 689–91 (2010). [PubMed: 20818861]
7. Minamino T and Komuro I, Regeneration of the endothelium as a novel therapeutic strategy for acute lung injury. J Clin Invest. 116, 2316–9 (2006). [PubMed: 16955131]
8. Angus DC, Linde-Zwirble WT, Lidicker J, Clermont G, Carcillo J, and Pinsky MR, Epidemiology of severe sepsis in the United States: analysis of incidence, outcome, and associated costs of care. Crit Care Med. 29, 1303–1310 (2001). [PubMed: 11445675]
9. Gee MH, Gottlieb JE, Albertine KH, Kubis JM, Peters SP, and Fish JE, Physiology of aging related to outcome in the adult respiratory distress syndrome. J Appl Physiol. 69, 822–829 (1990). [PubMed: 2246169]
10. Griffith D and Idell S, Approach to adult respiratory distress syndrome and respiratory failure in elderly patients. Clin Chest Med. 14, 571–582 (1993). [PubMed: 8222570]
11. Sloane PJ, Gee MH, Gottlieb JE, Albertine KH, Peters SP, Burns JR, Machiedo G, and Fish JE, A multicenter registry of patients with acute respiratory distress syndrome. Am Rev Respir Dis. 146, 419–426 (1992). [PubMed: 1489134]
12. Clark KL, Halay ED, Lai E, and Burley SK, Co-crystal structure of the HNF-3/fork head DNA-recognition motif resembles histone H5. Nature. 364, 412–20 (1993). [PubMed: 8332212]
13. Kaestner KH, Knochel W, and Martinez DE, Unified nomenclature for the winged helix/forkhead transcription factors. Genes Dev. 14, 142–6 (2000). [PubMed: 10702024]
14. Laoukili J, Kooistra MR, Bras A, Kauw J, Kerkhoven RM, Morrison A, Clevers H, and Medema RH, FoxM1 is required for execution of the mitotic programme and chromosome stability. Nat Cell Biol. 7, 126–36 (2005). [PubMed: 15654331]
15. Wang IC, Chen YJ, Hughes D, Petrovic V, Major ML, Park HJ, Tan Y, Ackerson T, and Costa RH, Forkhead box M1 regulates the transcriptional network of genes essential for mitotic progression and genes encoding the SCF (Skp2-Cks1) ubiquitin ligase. Mol Cell Biol. 25, 10875–94 (2005). [PubMed: 16314512]
16. Ye H, Kelly TF, Samadani U, Lim L, Rubio S, Overdier DG, Roebuck KA, and Costa RH, Hepatocyte nuclear factor 3/fork head homolog 11 is expressed in proliferating epithelial and mesenchymal cells of embryonic and adult tissues. Mol Cell Biol. 17, 1626–41 (1997). [PubMed: 9032290]
17. Dai Z, Zhu MM, Peng Y, Jin H, Machireddy N, Qian Z, Zhang X, and Zhao YY, Endothelial and Smooth Muscle Cell Interaction via FoxM1 Signaling Mediates Vascular Remodeling and Pulmonary Hypertension. Am J Respir Crit Care Med. 198, 788–802 (2018). [PubMed: 29664678]

18. Hou Y, Li W, Sheng Y, Li L, Huang Y, Zhang Z, Zhu T, Peace D, Quigley JG, Wu W, Zhao YY, and Qian Z, The transcription factor Foxm1 is essential for the quiescence and maintenance of hematopoietic stem cells. Nat Immunol. 16, 810–8 (2015). [PubMed: 26147687]
19. Zhao YY, Gao XP, Zhao YD, Mirza MK, Frey RS, Kalinichenko VV, Wang IC, Costa RH, and Malik AB, Endothelial cell-restricted disruption of FoxM1 impairs endothelial repair following LPS-induced vascular injury. J Clin Invest. 116, 2333–43 (2006). [PubMed: 16955137]
20. Zhao YD, Huang X, Yi F, Dai Z, Qian Z, Tiruppathi C, Tran K, and Zhao YY, Endothelial FoxM1 mediates bone marrow progenitor cell-induced vascular repair and resolution of inflammation following inflammatory lung injury. Stem Cells. 32, 1855–64 (2014). [PubMed: 24578354]
21. Mirza MK, Sun Y, Zhao YD, Potula HH, Frey RS, Vogel SM, Malik AB, and Zhao YY, FoxM1 regulates re-annealing of endothelial adherens junctions through transcriptional control of beta-catenin expression. J Exp Med. 207, 1675–85 (2010). [PubMed: 20660612]
22. Liu Y, Sadikot RT, Adami GR, Kalinichenko VV, Pendyala S, Natarajan V, Zhao YY, and Malik AB, FoxM1 mediates the progenitor function of type II epithelial cells in repairing alveolar injury induced by Pseudomonas aeruginosa. J Exp Med. 208, 1473–84 (2011). [PubMed: 21708928]
23. Wang X, Kiyokawa H, Dennewitz MB, and Costa RH, The Forkhead Box m1b transcription factor is essential for hepatocyte DNA replication and mitosis during mouse liver regeneration. Proc Natl Acad Sci U S A. 99, 16881–6 (2002). [PubMed: 12482952]
24. Fujita M, Kuwano K, Kunitake R, Hagimoto N, Miyazaki H, Kaneko Y, Kawasaki M, Maeyama T, and Hara N, Endothelial cell apoptosis in lipopolysaccharide-induced lung injury in mice. Int Arch Allergy Immunol. 117, 202–8 (1998). [PubMed: 9831808]
25. Kitamura Y, Hashimoto S, Mizuta N, Kobayashi A, Kooguchi K, Fujiwara I, and Nakajima H, Fas/FasL-dependent apoptosis of alveolar cells after lipopolysaccharide-induced lung injury in mice. Am J Respir Crit Care Med. 163, 762–9 (2001). [PubMed: 11254536]
26. Buras JA, Holzmann B, and Sitkovsky M, Animal models of sepsis: setting the stage. Nat Rev Drug Discov. 4, 854–65 (2005). [PubMed: 16224456]
27. Rittirsch D, Huber-Lang MS, Flierl MA, and Ward PA, Immunodesign of experimental sepsis by cecal ligation and puncture. Nat Protoc. 4, 31–6 (2009). [PubMed: 19131954]
28. Kalinichenko VV, Gusarova GA, Tan Y, Wang IC, Major ML, Wang X, Yoder HM, and Costa RH, Ubiquitous expression of the forkhead box M1B transgene accelerates proliferation of distinct pulmonary cell types following lung injury. J Biol Chem. 278, 37888–94 (2003). [PubMed: 12867420]
29. Zhang X, Jin H, Huang X, Chaurasiya B, Dong D, Shanley TP, and Zhao YY. Robust genome editing in adult vascular endothelium by nanoparticle delivery of CRISPR/Cas9 plasmid DNA. Cell Reports. 38, 110196 (2022). [PubMed: 34986352]
30. Huang X, Dai Z, Cai L, Sun K, Cho J, Albertine KH, Malik AB, Schraufnagel DE, and Zhao YY, Endothelial p110gammaPI3K Mediates Endothelial Regeneration and Vascular Repair After Inflammatory Vascular Injury. Circulation. 133, 1093–103 (2016). [PubMed: 26839042]
31. De Backer D, Creteur J, Preiser JC, Dubois MJ, and Vincent JL, Microvascular blood flow is altered in patients with sepsis. Am J Respir Crit Care Med. 166, 98–104 (2002). [PubMed: 12091178]
32. Han S, Lee SJ, Kim KE, Lee HS, Oh N, Park I, Ko E, Oh SJ, Lee YS, Kim D, Lee S, Lee DH, Lee KH, Chae SY, Lee JH, Kim SJ, Kim HC, Kim S, Kim SH, Kim C, Nakaoka Y, He Y, Augustin HG, Hu J, Song PH, Kim YI, Kim P, Kim I, and Koh GY, Amelioration of sepsis by TIE2 activation-induced vascular protection. Sci Transl Med. 8, 335ra55 (2016).
33. Trzeciak S, Dellinger RP, Parrillo JE, Guglielmi M, Bajaj J, Abate NL, Arnold RC, Colilla S, Zanotti S, Hollenberg SM, Microcirculatory Alterations in R, and Shock I, Early microcirculatory perfusion derangements in patients with severe sepsis and septic shock: relationship to hemodynamics, oxygen transport, and survival. Ann Emerg Med. 49, 88–98, 98 e1–2 (2007). [PubMed: 17095120]
34. Gill SE, Rohan M, and Mehta S, Role of pulmonary microvascular endothelial cell apoptosis in murine sepsis-induced lung injury in vivo. Respir Res. 16, 109 (2015). [PubMed: 26376777]

35. Wang HL, Akinci IO, Baker CM, Urich D, Bellmeyer A, Jain M, Chandel NS, Mutlu GM, and Budinger GR, The intrinsic apoptotic pathway is required for lipopolysaccharide-induced lung endothelial cell death. J Immunol. 179, 1834–41 (2007). [PubMed: 17641050]
36. Mao SZ, Ye X, Liu G, Song D, and Liu SF, Resident Endothelial Cells and Endothelial Progenitor Cells Restore Endothelial Barrier Function After Inflammatory Lung Injury. Arterioscler Thromb Vasc Biol. 35, 1635–1644 (2015). [PubMed: 25977568]
37. Koni PA, Joshi SK, Temann UA, Olson D, Burkly L, and Flavell RA, Conditional vascular cell adhesion molecule 1 deletion in mice: impaired lymphocyte migration to bone marrow. J Exp Med. 193, 741–54 (2001). [PubMed: 11257140]
38. Liu M, Zhang L, Marsboom G, Jambusaria A, Xiong S, Toth PT, Benevolenskaya EV, Rehman J, and Malik AB, Sox17 is required for endothelial regeneration following inflammation-induced vascular injury. Nat Commun. 10, 2126 (2019). [PubMed: 31073164]
39. Docherty AB, Harrison EM, Green CA, Hardwick HE, Pius R, Norman L, Holden KA, Read JM, Dondelinger F, Carson G, Merson L, Lee J, Plotkin D, Sigfrid L, Halpin S, Jackson C, Gamble C, Horby PW, Nguyen-Van-Tam JS, Ho A, Russell CD, Dunning J, Openshaw PJ, Baillie JK, Semple MG, and investigators IC, Features of 20 133 UK patients in hospital with covid-19 using the ISARIC WHO Clinical Characterisation Protocol: prospective observational cohort study. BMJ. 369, m1985 (2020). [PubMed: 32444460]
40. Salje H, Tran Kiem C, Lefrancq N, Courtejoie N, Bosetti P, Paireau J, Andronico A, Hoze N, Richet J, Dubost CL, Le Strat Y, Lessler J, Levy-Bruhl D, Fontanet A, Opatowski L, Boelle PY, and Cauchemez S, Estimating the burden of SARS-CoV-2 in France. Science. 369, 208–211 (2020). [PubMed: 32404476]
41. Thangavel J, Malik AB, Elias HK, Rajasingh S, Simpson AD, Sundivakkam PK, Vogel SM, Xuan YT, Dawn B, and Rajasingh J, Combinatorial therapy with acetylation and methylation modifiers attenuates lung vascular hyperpermeability in endotoxemia-induced mouse inflammatory lung injury. Am J Pathol. 184, 2237–49 (2014). [PubMed: 24929240]
42. Liu Y, Sadikot RT, Adami GR, Kalinichenko VV, Pendyala S, Natarajan V, Zhao YY, Malik AB. FoxM1 mediates the progenitor function of type II epithelial cells in repairing alveolar injury induced by Pseudomonas aeruginosa. J Exp Med. 208, 1473–1484 (2011). [PubMed: 21708928]
43. Gothert JR, Gustin SE, van Eekelen JA, Schmidt U, Hall MA, Jane SM, Green AR, Gottgens B, Izon DJ, and Begley CG, Genetically tagging endothelial cells in vivo: bone marrow-derived cells do not contribute to tumor endothelium. Blood. 104, 1769–77 (2004). [PubMed: 15187022]
44. Tran KA, Zhang X, Predescu D, Huang X, Machado RF, Gothert JR, Malik AB, Valyi-Nagy T, and Zhao YY, Endothelial beta-Catenin Signaling Is Required for Maintaining Adult Blood-Brain Barrier Integrity and Central Nervous System Homeostasis. Circulation. 133, 177–86 (2016). [PubMed: 26538583]
45. Huang X and Zhao YY, Transgenic expression of FoxM1 promotes endothelial repair following lung injury induced by polymicrobial sepsis in mice. PLoS One. 7, e50094 (2012). [PubMed: 23185540]
46. Li LC, Dahiya R, MethPrimer: designing primers for methylation PCRs. Bioinformatics. 18, 1427–1431 (2002). [PubMed: 12424112]
47. Wojdacz TK, Dobrovic A, Hansen LL, Methylation-sensitive high-resolution melting. Nat Protoc. 3, 1903–1908 (2008). [PubMed: 19180074]
48. Dai Z, Zhu MM, Peng Y, Qian Z, Zhang X, and Zhao YY. Endothelial and Smooth Muscle Cell Interaction via FoxM1 Signaling Mediates Vascular Remodeling and Pulmonary Hypertension. Am J Respir Crit Care Med. 198, 788–802 (2018). [PubMed: 29664678]

OVERLINE: LUNG INJURY

One sentence summary:

Decitabine treatment or nanoparticle delivery of the *FOXM1* gene reactivates intrinsic endothelial regeneration in the lungs of aged septic mice.

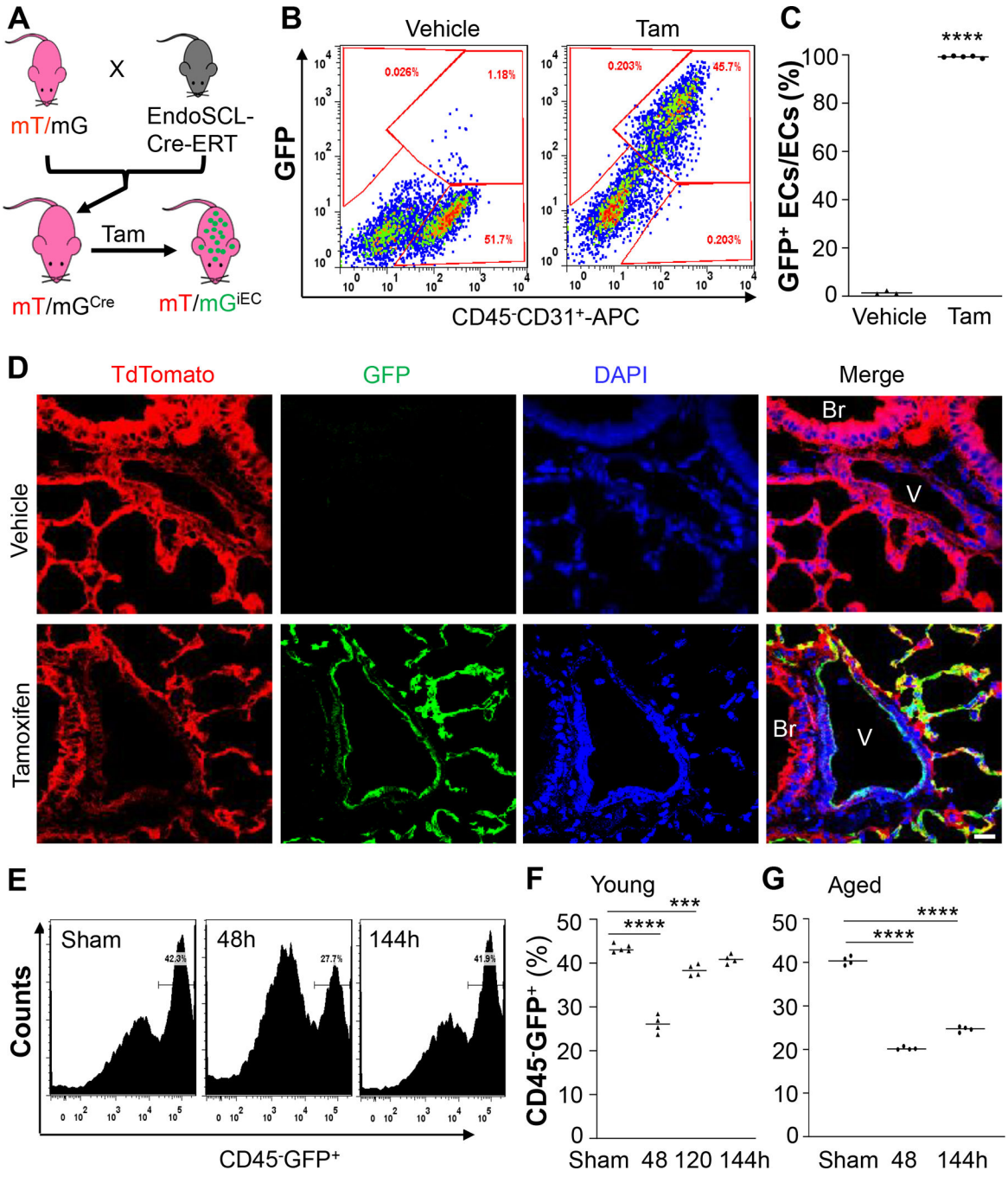

Fig. 1. Genetic lineage tracing of ECs after polymicrobial sepsis-induced injury.

(A) Schematic illustration of the lineage-tracing strategy. Tam=Tamoxifen. **(B)** Flow cytometry analysis of GFP^+ cells and ECs ($CD45^-CD31^+$) in lungs of young adult mice. **(C)** Quantification of lung GFP^+ ECs in young adult *EndoSCL*-Cre^{ERT2}/mTmG mice. $CD45^-$ cells were gated for $CD31^+$ and GFP^+ analysis. **(D)** Representative confocal images of lungs of young adult mice showing tamoxifen treatment-induced EC labeling. Green, GFP; Red, tdTomato; Blue, DAPI. Br, bronchiole; V, vessel. Scale bar, 20 μm. (**E** and **F**) FACS analysis of GFP^+ ECs at 48h and 144h in young adult mice. Lung cells were $CD45^-$ gated, and GFP^+

population were quantified. **(G)** FACS analysis showing impaired recovery of lung GFP^+ cells following CLP challenge in aged mice (19–21 mos. old). Bars represent means. ***$P <$ 0.001, ****$P < 0.0001$. Unpaired two-tailed t test (**C**); One-way ANOVA (Dunnett) (**F**, **G**).

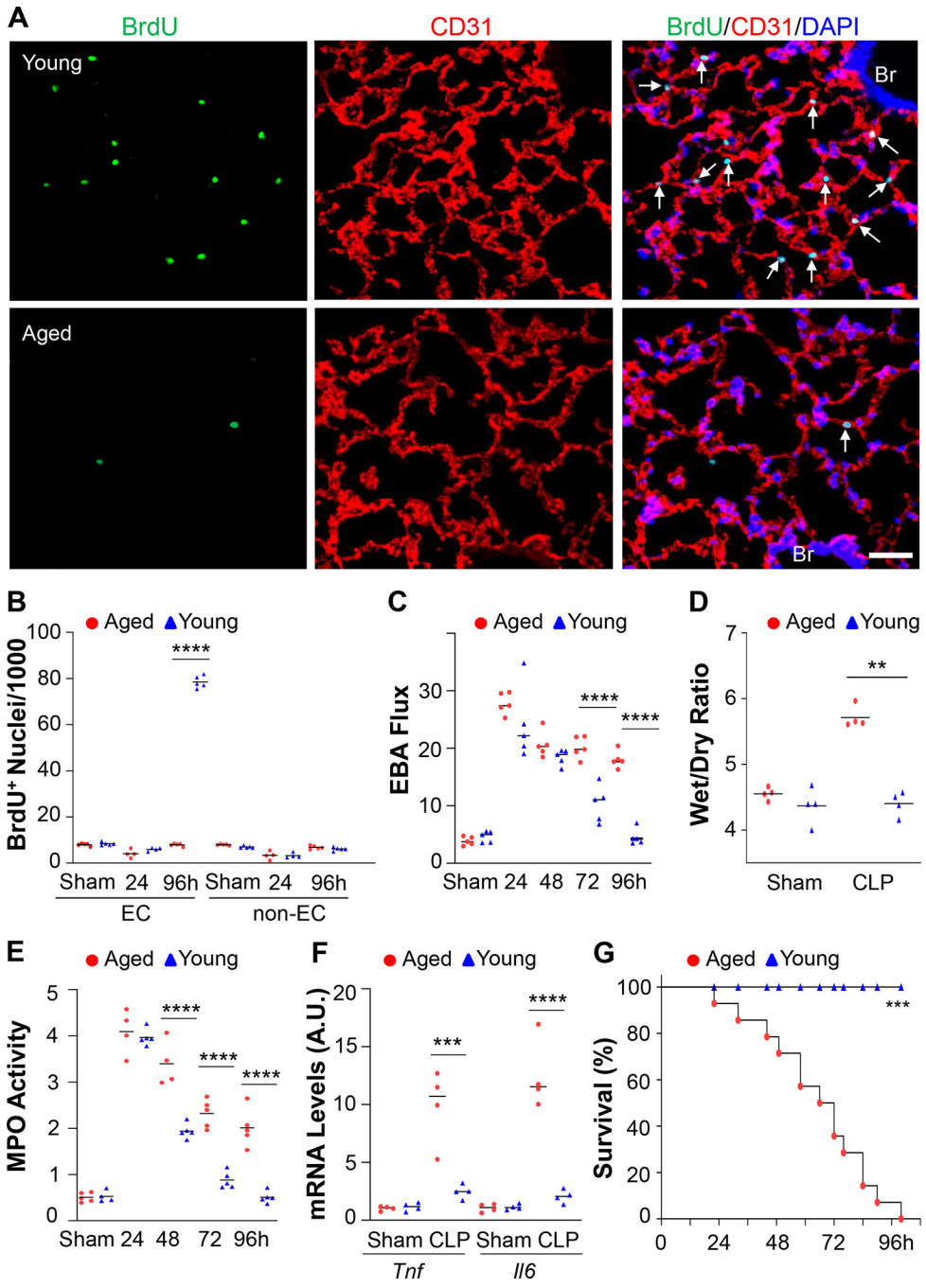

Fig. 2. Defective endothelial proliferation and vascular repair in aged lungs following polymicrobial sepsis in mice.

(**A**) Representative micrographs of BrdU immunostaining showing defective EC proliferation in aged lungs. Cryosections of lungs (5 μm) collected at 96h after CLP were immunostained with anti-BrdU antibody to identify proliferating cells (green) and with anti-CD31 antibody to identify ECs (red). Nuclei were counterstained with DAPI (blue). Arrows point to proliferating ECs. Aged, 20 mos. old; young, 3 mos. old; Scale bar, 50 μm. (**B**) Quantification of cell proliferation in mouse lungs. Three consecutive cryosections from

each mouse lung were examined, the average number of $BrdU^+$ nuclei was used. (**C**) Lung vascular permeability assessed by an EBA extravasation assay. Lung tissues of aged mice were collected at indicated times after CLP for EBA assay. (**D**) Lung wet/dry weight ratio. At 96h after CLP, lung tissues were collected and dried at 60°C for 3 days for calculation of wet/dry ratio. (**E**) MPO activities in lung tissues at the indicated timepoints after CLP. MPO activity was calculated as OD_{460}/min/g lung tissue. **(F)** QRT-PCR analysis showing marked increase of expression of proinflammatory genes *Tnf* and *Il6* in lungs of aged mice at 96h after CLP compared to young mice. A.U., arbitrary units. (**G**) Survival rates of young (3.5 mos.) and aged (21 mos.) mice after CLP. $^{**}P < 0.01$; $^{***}P < 0.001$, $^{****}P < 0.0001$. One-way ANOVA (Tukey) (B, C, E, F); Kruskal-Wallis (D). Log-rank (Mantel-Cox) test (**G**).

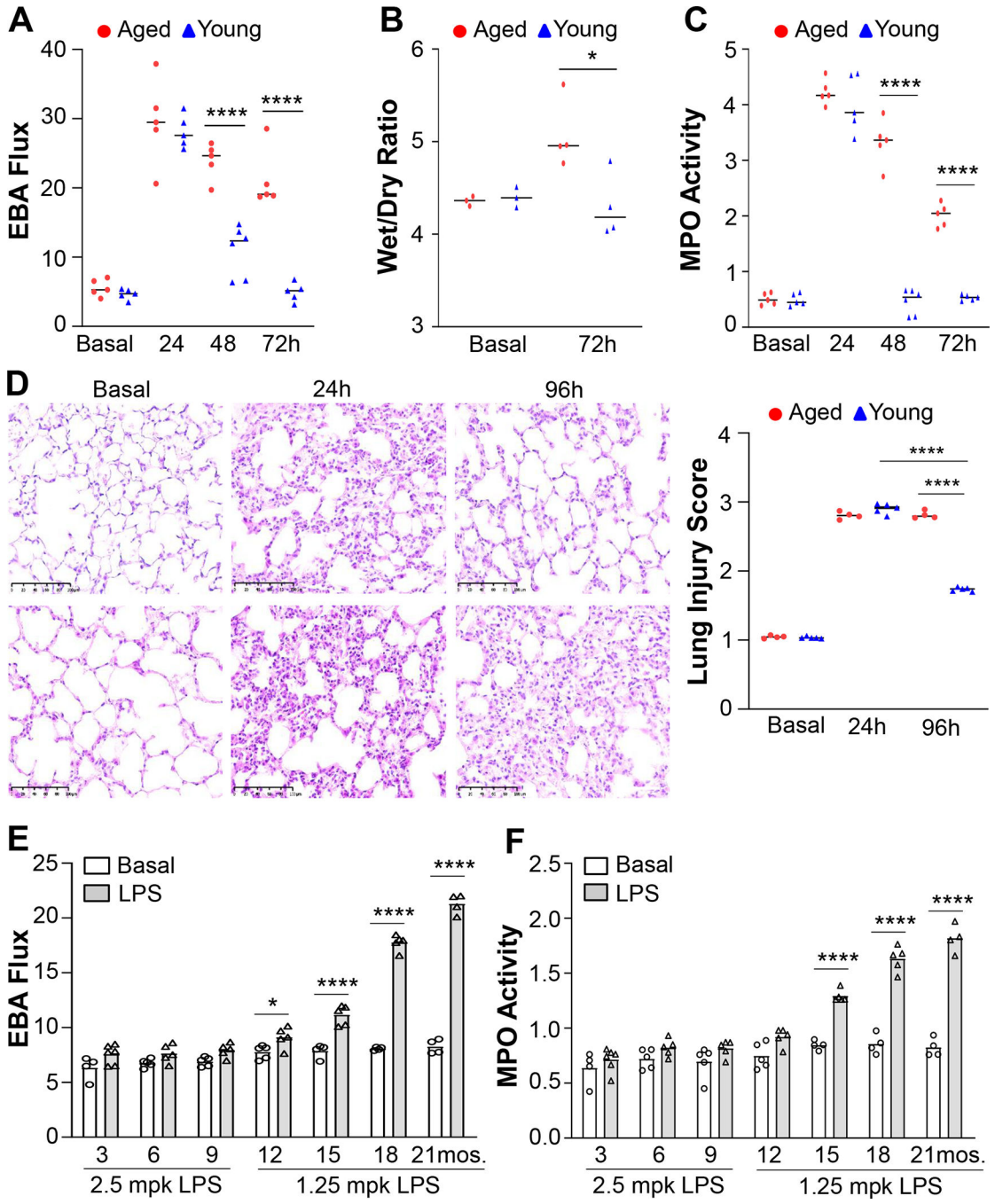

Fig. 3. Aging impairs vascular repair and resolution of inflammatory lung injury in mice after LPS challenge.

(**A**) Lung vascular permeability assessed by an EBA extravasation assay of young and aged mice at the indicated timepoints after LPS challenge (i.p.). Young adult mice (3–5 mos.) were challenged with 2.5 mg/kg of LPS whereas aged mice (19–21 mos.) were challenged with 1.0 mg/kg of LPS. (**B**) Lung wet/dry ratios in young adult and aged mice at 72h after LPS. (**C**) MPO activity in young adult and aged lungs at the indicated timepoints after LPS challenge. (**D**) Representative micrographs of H &E staining and quantification of lung

injury. Based on inflammatory cell infiltration, alveolus edema and septal thickening, each section area was assigned to an injury score from 1(normal) to 4 (severe injury) and the size of the area was quantified. Lung injury score was calculated by the sum of the percentage of the area size × its respective injury score. Scale bar 40 μm. (**E**) EBA flux assay in the lungs of mice at different ages, before and after LPS challenge. WT mice at indicated ages were challenged with LPS (mice at age of 3–9 mos. with 2.5 mg/kg, and at age of 12–21 mos. with 1.25 mg/kg LPS). At 72h after LPS, lungs were collected for EBA extravasation assay. (**F**) Lung MPO activity in mice at various ages at 72h after LPS challenge. *$P < 0.05$; **$P < 0.01$; ****$P < 0.0001$. Kruskal-Wallis (A); One-way ANOVA (B-D); Two-way ANOVA (Sidak) (**E-F**).

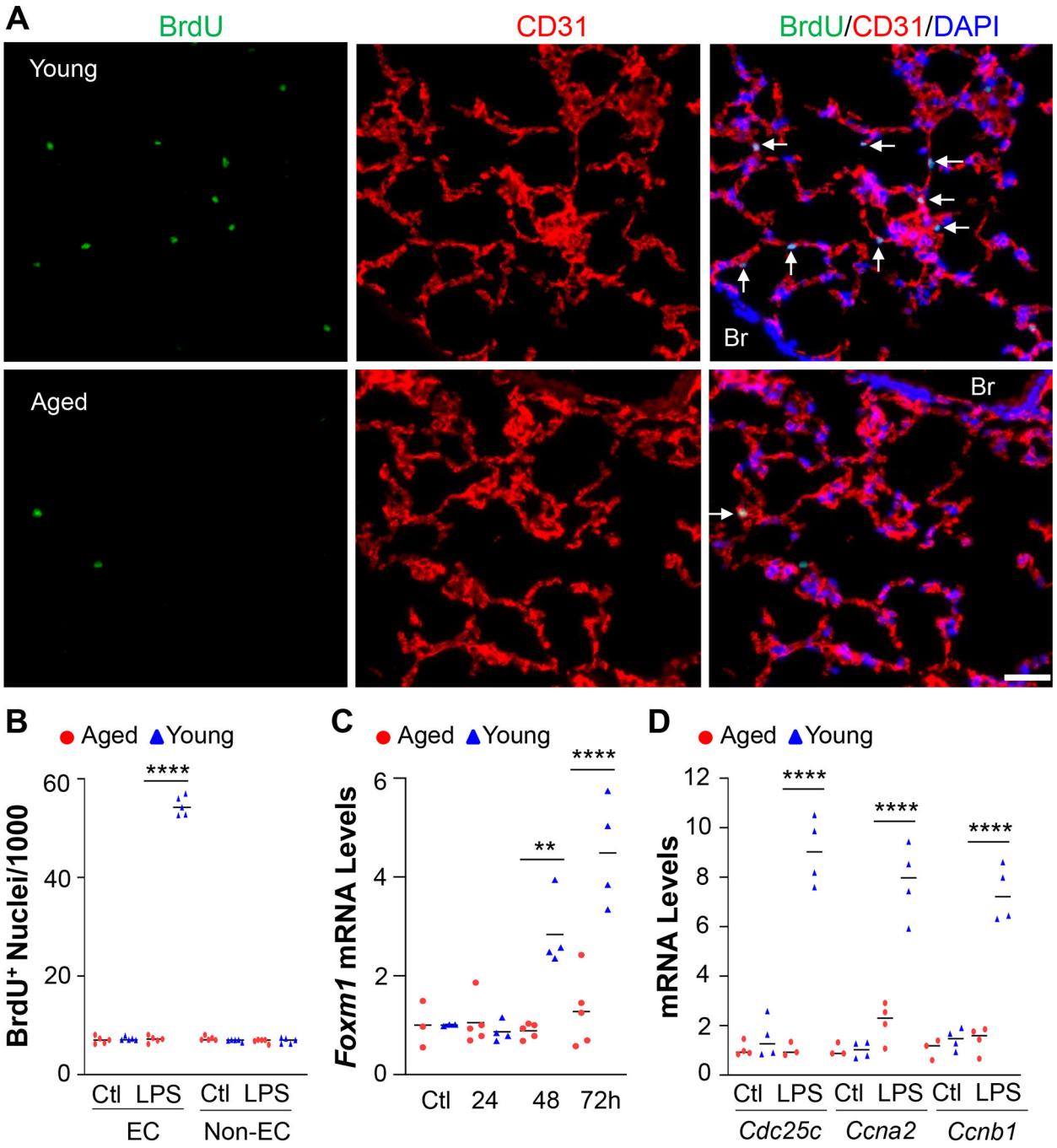

Fig. 4. Reduced endothelial proliferation and FoxM1 induction in aged lungs after LPS challenge in mice.

(**A**) Representative micrographs of immunostaining showing inhibited endothelial proliferation in lungs of aged mice (20 mos.) at 72h post-LPS. Lung cryosections were immunostained with anti-BrdU (green), and anti-CD31 (red, ECs). Nuclei were counterstained with DAPI (blue). White arrows point to proliferating ECs. Br = bronchiole. Scale bar, 50 μm. (**B**) Quantification of cell proliferation in mouse lungs at baseline (Ctl) and 72h after LPS. (**C**) QRT-PCR analysis of *Foxm1* expression in mouse lungs at indicated

times after LPS. (**D**) QRT-PCR analysis of expression of genes *Cdc25c*, *Ccna2*, and *Ccnb1* at 72h after LPS in the lungs of young mice and aged mice. $^{**}P < 0.01$; $^{***}P < 0.001$; $^{****}P < 0.0001$. One-way ANOVA (Tukey).

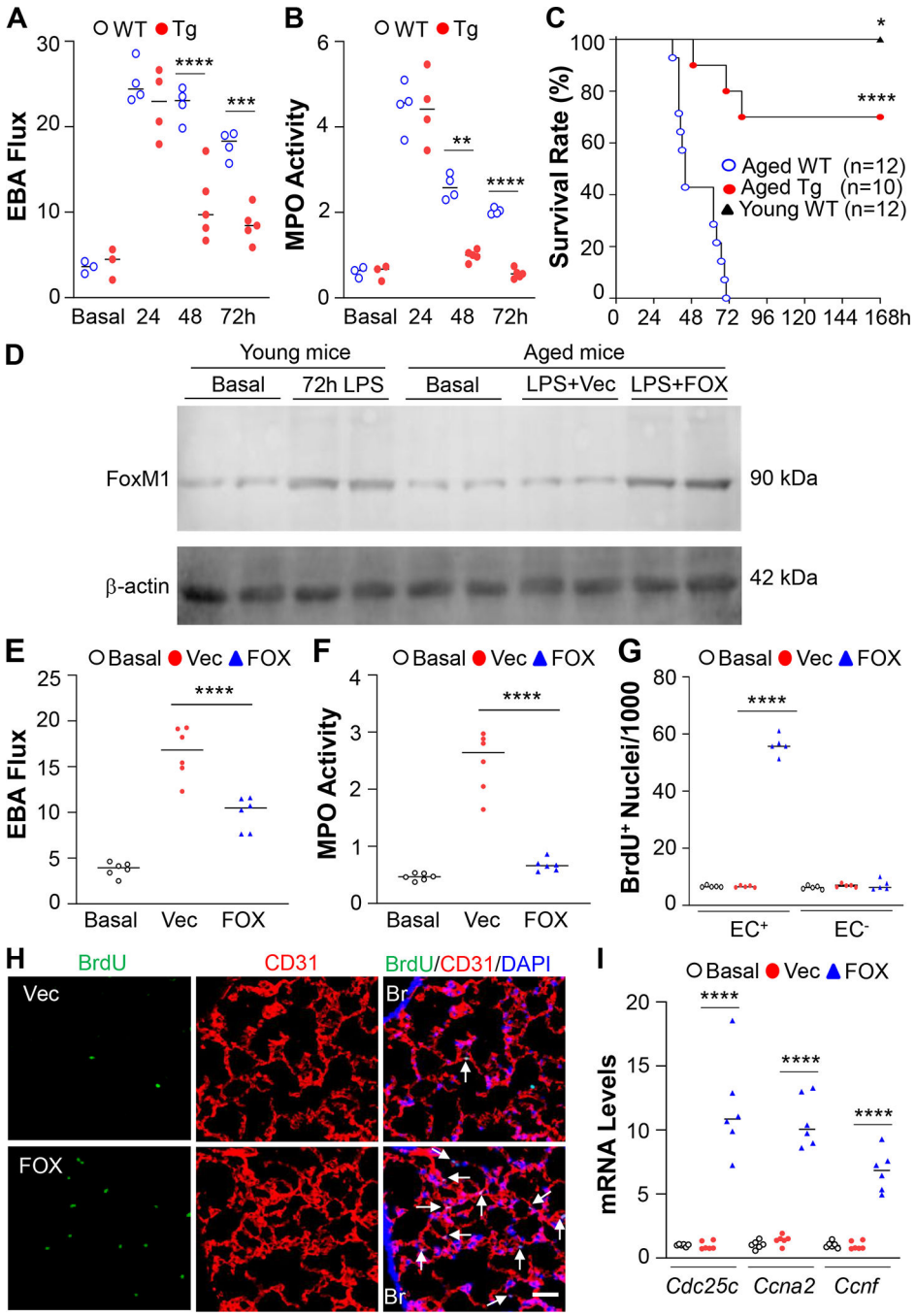

Fig. 5. Forced expression of FoxM1 improves resolution of inflammatory lung injury and promotes survival of aged mice.

(**A**) EBA flux assay in 20-month-old WT and *FOXM1*^{Tg} mice challenged with LPS (1 mg/kg, i.p.). (**B**) Lung MPO activity in aged WT and aged *FOXM1*^{Tg} mice. (**C**) Kaplan-Meier survival curves after LPS challenge. WT mice at age of 3–5 (Young WT), or 21 mos. (Aged WT), and aged *FOXM1*^{Tg} mice (21 mos.) were challenged with 1.5 mg/kg of LPS (i.p.). Survival rates were recorded for 7 days. (**D**) Representative Western blotting demonstrating FoxM1 expression in lungs of aged WT mice administered with *FOXM1*

plasmid DNA (FOX) compared to empty vector (Vec). Mixture of nanoparticles with *FOXM1* plasmid DNA (*CDH5* promoter) or empty vector DNA (Vec) were administered retro-orbitally to aged WT mice at 24h after LPS (1mg/kg, i.p.). Lungs were collected at 72h after LPS. Basal, mice without plasmid DNA and LPS. (**E**EBA flux in *FOXM1* plasmid-administered mice at 72h after LPS compared to vector mice. (**F**) MPO activity assay in vector- and FOXM1 plasmid-adminsitered aged mice at 72h after LPS. (**G**) Quantification of $BrdU^+$ nuclei of $CD31^+$ (ECs) and $CD31^-$ (non-ECs) cells in mouse lungs at baseline and 72h after LPS. (**H**) Representative micrographs of anti-BrdU immunostaining (green) of mouse lungs collected at 72h after LPS. ECs were immunostained with anti-CD31 (red). Nuclei were counterstained with DAPI (blue). White arrows point to proliferating ECs. Scale bar, 50 μm. (**I**) QRT-PCR analysis of FoxM1 target genes *Cdc25c*, *Ccna2*, and *Ccnf*. $*P < 0.05$; $**P < 0.01$; $***P < 0.001$; $****P < 0.0001$. One-way ANOVA (Tukey) (**A**, **B,** **E-I**). Log-rank (Mantel-Cox) test (**C**).

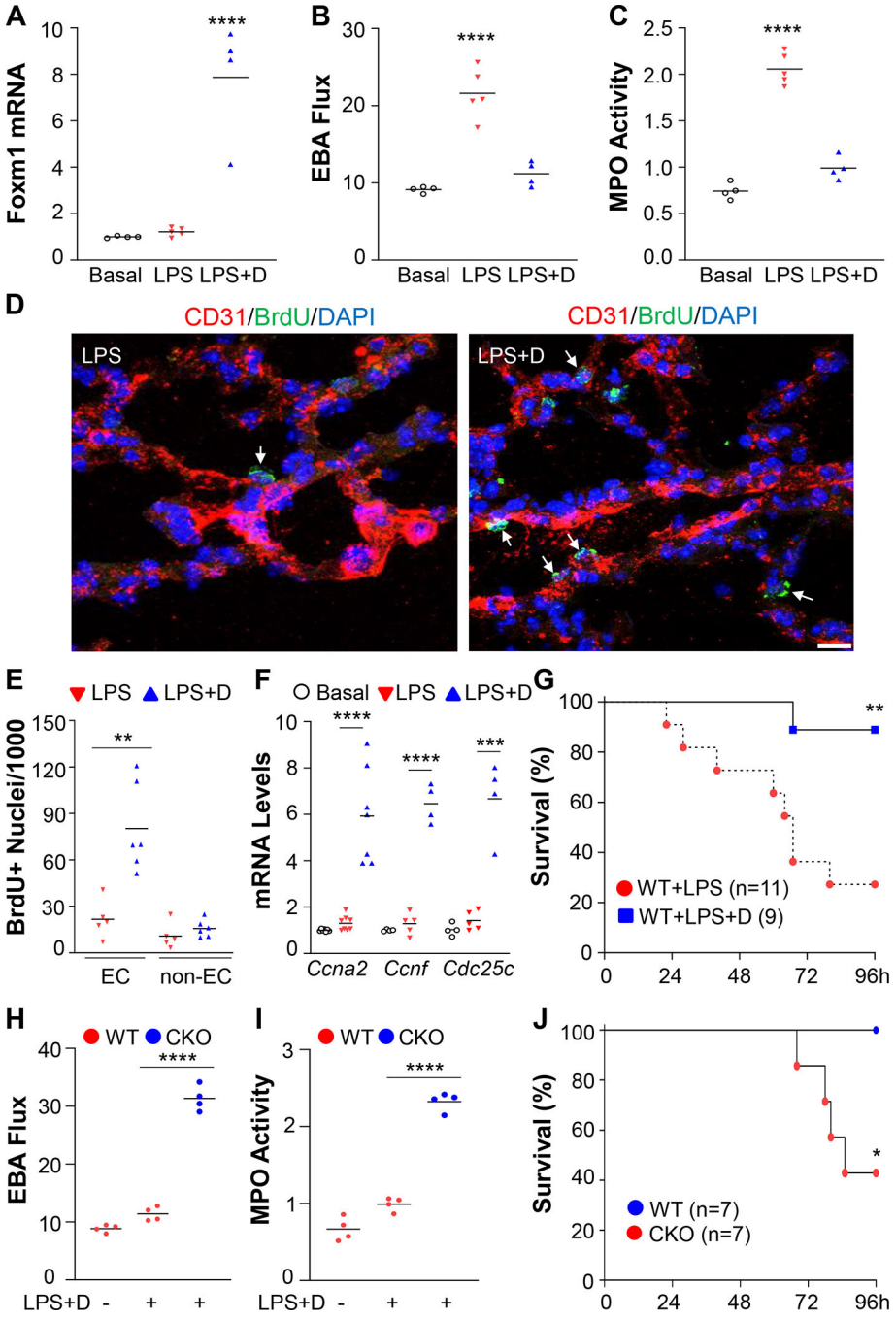

Fig. 6. Therapeutic activation of FoxM1-dependent endothelial regeneration by decitabine improves resolution of inflammatory lung injury and promotes survival of aged WT mice.

(**A**) QRT-PCR analysis demonstrating induction of *FOXM1* expression in lungs of aged WT mice after decitabine treatment. 21 mos. old WT mice were challenged with LPS (1.0 mg/kg, i.p.) and then treated with either decitabine (0.2mg/kg, oral gavage) (LPS+D) or PBS (LPS) once daily at 24 and 48h after LPS. Lung tissues were collected at 96h after LPS for assays. (**B**) EBA flux assay in aged WT mice treated with decitabine or PBS after exposure to LPS. (**C**) Lung MPO activity assessment. (**D**) Representative micrographs of

anti-BrdU staining. Lung sections were immunostained with anti-CD31 (red) and anti-BrdU (green). Nuclei were counterstained with DAPI (blue). Arrows point to $BrdU^+$ ECs. Scale bar, 20 μm. (**E**) Quantification of $BrdU^+$ ECs and non-ECs in mouse lungs. (**F**) QRT-CPR analysis of FoxM1 target genes in mouse lungs. (**G**) Kaplan-Meier survival curves of aged WT mice (21 mos.) after LPS (1.5 mg/kg, i.p.) and treated with either PBS or decitabine. (**H, I**) Lung vascular permeability assessed by an EBA extravasation assay (**H**) and lung MPO activities (**I**) in aged *Foxm1 CKO* (CKO) mice. 24 mos. old WT or *Foxm1 CKO* mice were challenged with 0.3 mg/kg LPS followed by Decitabine treatment at 24 and 48h. Lung tissues were collected at 96h post-LPS for EBA (**H**) and MPO (**I**) assays. (**J**) Kaplan-Meier survival curves of aged WT and *Foxm1 CKO* (CKO) mice after LPS challenge. 20 mos. old WT and *Foxm1 CKO* mice were challenged with LPS (1.5 mg/kg, i.p.) and then treated with decitabine at 24 and 48h post-LPS. $*P < 0.05$; $**P < 0.01$; $***P < 0.001$; $****P < 0.0001$. One-way ANOVA (Tukey) (**A-C, H, I**); Unpaired two-tailed t test (**E, F**); **Log-**rank (Mantel-Cox) test (**G, J**).

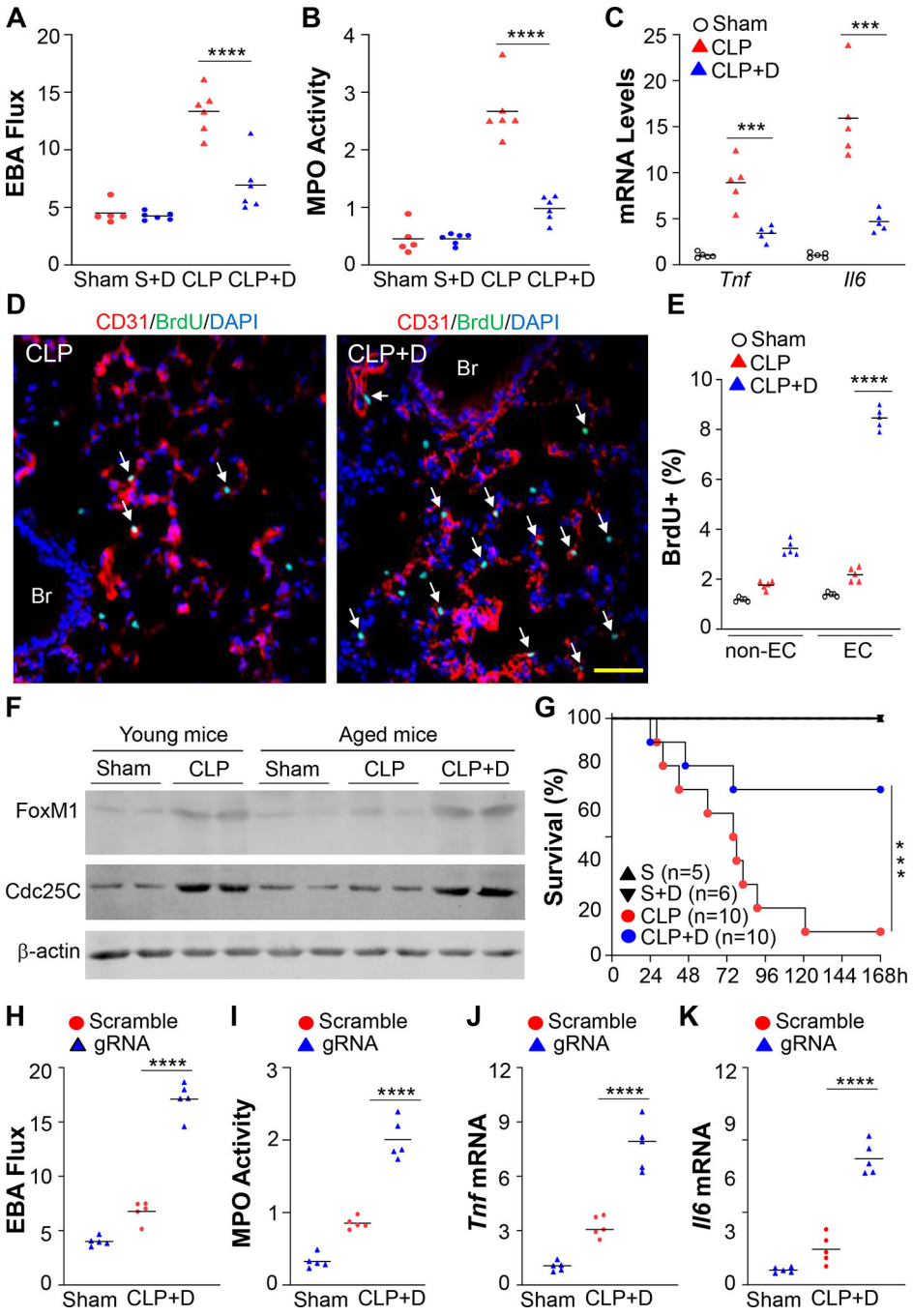

Fig. 7. Decitabine treatment promotes FoxM1-mediated vascular repair and resolution of inflammatory lung injury after polymicrobial sepsis in mice.

20–21 mos. old WT mice were challenged with either CLP or sham surgery and then treated with decitabine (D) or PBS at 24 and 48h post-CLP. Lung tissues were collected at 96h after CLP. S+D=Sham+decitabine. (**A**) Lung vascular permeability assessed by an EBA extravasation assay. (**B**) lung MPO activities. (**C**) Quantitative RT-PCR analysis of *Tnf* and *Il6* gene expression. (**D**) Representative micrographs of anti-BrdU immunostaining (green) of lung cryosections. ECs were immunostained with anti-CD31 (red). Nuclei were

counterstained with DAPI (blue). White arrows point to proliferating ECs. Br = Bronchiole. Scale bar, 50 μm. (**E**) Quantification of $BrdU^+$ nuclei. (**F**) Western blotting demonstrating expression of FoxM1 and Cdc25C in lungs of aged mice after sham surgery or CLP and treatment with decitabine. (**G**) Survival rates of aged WT mice after CLP. S=Sham, S+D=Sham+D. (**H**) Lung vascular permeability assessed by an EBA extravasation. 20 months old WT mice were administered retro-orbitally with mixture of nanoparticle:plasmid DNA expressing Cas9 under the control of *CDH5* promoter and guide RNA (gRNA) or scrambled RNA (Scramble) driven by *U6* promoter and 7 days later, the mice were subjected to Sham or CLP followed by decitabine treatment at 24 and 48h post-CLP (CLP+D). At 96h post-CLP, lung tissues were collected for EBA assay. (**I-K**) Lung MPO activity (**I**) and expression of *Tnf* and *Il6* analyzed by qRT-PCR (**J, K**). ***$P < 0.001$; ****$P < 0.0001$. One-way ANOVA (Tukey) (**A-C**, **E**, **F**, **H-K**); Log-rank (Mantel-Cox) test (**G**).

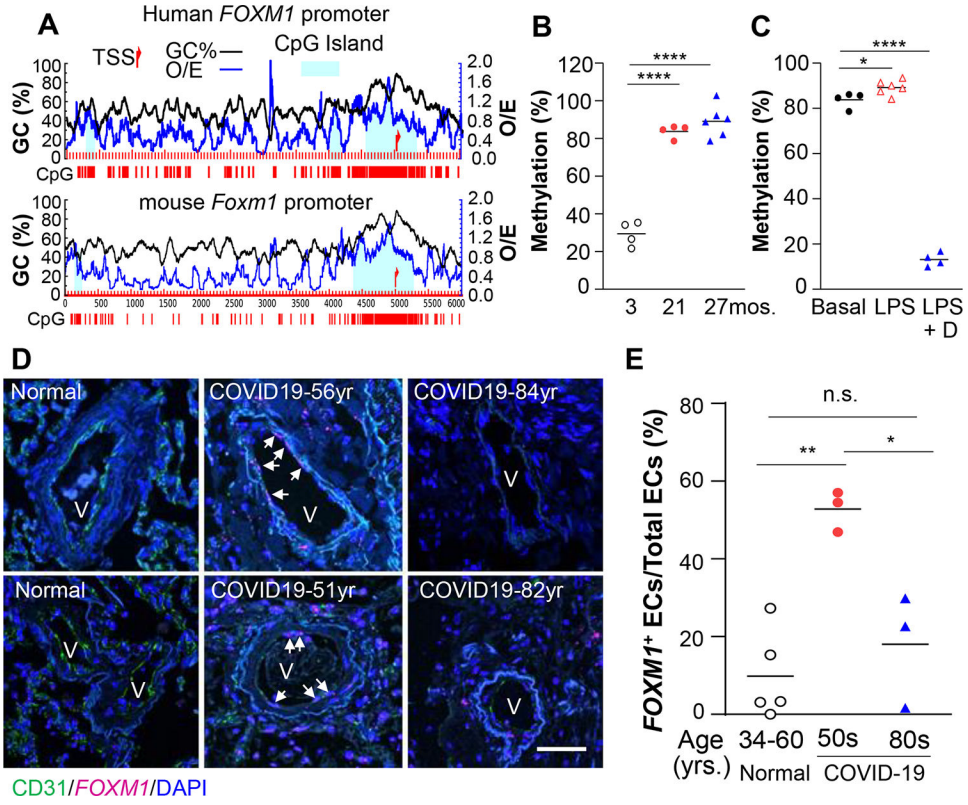

Fig. 8. Aging impaired FoxM1 expression in mice and human through hypermethylation of the promoter.

(**A**) Diagram presentation of MethPrimer analysis of human *FOXM1* and mouse *Foxm1* promoter showing a predicted conserved CpG island near the transcription start site (TSS). O/E, Observed versus Expected. (**B**) Methylation-specific high-resolution DNA melting assay of the *Foxm1* promoter in lungs of aged mice compared to young mice at baseline. (**C**) Methylation-specific high-resolution DNA melting assay of the *Foxm1* promoter in lungs of aged mice (21 mos.) challenged with LPS. (**D**) Representative micrographs of RNAscope in situ hybridization staining of human lung sections showing induction of *FOXM1* expression in vascular ECs of middle-aged (50–60 years of age) COVID-19 patients but not in elderly (over 80 years old) patients. Lung autopsy tissues were collected from patients with COVID-19 and unused healthy donor lungs (normal) for paraffin-sectioning and immunostaining. Anti-CD31 antibody was used to immunostain ECs (green). *FOXM1* mRNA expression (purple) was detected by RNAscope in situ hybridization. Nuclei were counterstained with DAPI (blue). White arrows point to *FOXM1* expressing ECs. V, vessel. Scale bar, 50 μm. (**E**) Quantification of endothelial expression of *FOXM1*. *FOXM1* expressing ECs per vessel (endothelial $FOXM1^+$ nuclei/total endothelial nuclei of each vessel) was quantified in 15–33 vessels of each sample. Bars represent means. $*P < 0.05$; $**P < 0.01$; $****P < 0.0001$, One-way ANOVA (Tukey) (**B, C**, **E**).